Efficiency analysis of ignition by Nanosecond Repetitively Pulsed discharges using a low-order model

Stéphane Q.E. Wang, Yacine Bechane, Nasser Darabiha, Benoît Fiorina

Applications in Energy and Combustion Science 15 (2023) 100166

Contents lists available at ScienceDirect

Applications in Energy and Combustion Science

journal homepage: www.elsevier.com/locate/jaecs

Efficiency analysis of ignition by Nanosecond Repetitively Pulsed discharges using a low-order model

Stéphane Q.E. Wang, Yacine Bechane, Nasser Darabiha, Benoît Fiorina *

Université Paris-Saclay, CNRS, CentraleSupélec, Laboratoire EM2C, Gif-sur-Yvette 91190, France

ARTICLE INFO

Keywords:
Plasma-assisted combustion
Nanosecond Repetitively Pulsed discharges
Perfectly-stirred reactor
Flame ignition

ABSTRACT

Plasma-assisted combustion is an interesting method to promote the ignition of a lean reactive mixture instead of conventional spark plugs. Especially, Nanosecond Repetitively Pulsed (NRP) discharges technique is an energy-efficient way to initiate and control combustion processes. Ignition success or failure results from the competition between the discharge energy accumulation, the gas residence time in the discharge region, and the combustion chemistry. Plasma-assisted ignition is modeled here by a Perfectly-Stirred Reactor (PSR) whose volume represents the one surrounding the interelectrode region. NRP discharges are applied inside the reactor to initiate the combustion of the injected mixture. This model numerically identifies a plasma-assisted ignition efficiency map in terms of the amount of energy per pulse and the pulse repetition frequency, at low CPU cost. A criterion based on the residence time, interpulse time, and chemical time is introduced to predict the successful formation of a reactive kernel. This criterion is successfully validated by analyzing the plasma-assisted PSR solutions.

1. Introduction

Plasma-assisted combustion is an interesting method to promote the ignition of a lean reactive mixture instead of conventional spark plugs [1]. Among all investigated plasma-assisted technologies [1,2], Nanosecond Repetitively Pulsed (NRP) discharges techniques have been shown [3–9] to be a very energy-efficient way to initiate and control combustion processes. By applying a series of repetitive discharges, NRP discharges locally increase the gas temperature and generate active species [10]. In typical conditions, around 35% of molecular oxygen is dissociated to O radicals by the plasma discharge in the interelectrode region [10,11]. This high concentration of O radical positively affects the ignition phenomena [6], explaining the high efficiency of NRP discharges.

Mechanisms of plasma-assisted ignition by NRP discharges have been extensively investigated by Lefkowitz et al. [12–14] in a flow tunnel experimental device. Different pulses interactions mechanisms leading to ignition success or failure have been identified depending on the operating conditions.

The analysis of these experimental data and the conclusions obtained from the simulations of plasma-assisted ignition [15,16] suggest that ignition success or failure results from a competition between the time scales of pulse repetition, flow mixing and combustion chemistry. Indeed, from one side, by locally increasing the gas temperature and producing active radicals, NRP discharges enhance the chemical activities. The repetitive nature of the pulse will promote the local accumulation of thermal and chemical effects. On the other side, the flow dynamics will limit the residence time of the reactive mixture in the interelectrode region, where the pulses accumulate. The ignition naturally fails when the residence time becomes smaller than the time needed for combustion. A way to enhance the NRP efficiency is to increase the amount of deposited energy per pulse. As the temperature increases and the amount of O_2 dissociated into O are linked to the deposited energy, the chemistry will be faster. An alternative is to enhance the accumulation effect by increasing the pulse repetition frequency. Recent numerical simulations of a reactive kernel formation by NRP discharges [16] show that Large Eddy Simulations (LES) capture well the complex interactions between plasma, combustion, and turbulence. However, as the CPU cost is very high, this approach is not feasible to conduct parametric studies.

The present work aims to provide low CPU cost modeling tools for engineers in charge of designing future plasma-assisted combustion chambers. Two complementary approaches are developed in this work. The first one is a theoretical analysis based on dimensionless numbers. The second one employs a series of 0-D Perfectly-Stirred Reactor (PSR) computations filling the gaps of the theoretical analysis.

The paper is organized as follows. The simplified theory of ignition by NRP discharges is presented in Section 2, while a low-order model

* Corresponding author.
E-mail address: benoit.fiorina@centralesupelec.fr (B. Fiorina).

https://doi.org/10.1016/j.jaecs.2023.100166
Received 23 March 2023; Received in revised form 16 June 2023; Accepted 22 June 2023
Available online 4 July 2023

based on PSR is introduced in Section 3. The numerical set-up is given in Section 4, while the results are analyzed in Section 5. In particular, the impacts of both pulse energy and pulse repetition frequency on ignition efficiency are discussed. This study leads to the identification of a plasma-assisted ignition efficiency map in terms of the amount of energy per pulse and the pulse repetition frequency for a wide range of residence time across the interelectrode volume.

2. Simplified theory of ignition by NRP discharges

NRP discharges are characterized by high voltage pulses (5 to 20 kV) that last a few nanoseconds and are repeated at frequencies of the order of some tens of kHz. In this work, the studied plasma is in the non-thermal spark discharge regime is considered, which corresponds to an energy deposition at each pulse of the order of 1 mJ [17,18]. In this regime, the plasma causes a simultaneous ultra-fast increase of gas temperature and O_2 dissociation into O radical. It is then followed by a slower gas heating process, which results from the relaxation of nitrogen vibrational states. The time evolution of the hot kernel morphology computed by a Direct Numerical Simulation (DNS) [15] is shown in Fig. 1 for pulse repetition frequency $f_p = 5$ kHz and energy deposited per pulse $E_p = 1.5$ mJ. The shape of the kernel, initially cylindrical, is deformed by a toroidal recirculating zone resulting from the expansion of the hot gases.

As the energy deposited per pulse is limited, a series of pulses is generally required to ignite the reactive mixture [12,16]. Ignition success or failure will therefore result from a competition between the two following phenomena:

- A cumulative energy deposition in the interelectrode region, which promotes ignition. The amount of deposited energy is controlled by the pulse repetition frequency f_p and the energy per pulse E_p.
- The evacuation of the hot gases outside the interelectrode region and the fresh gases renewal by the toroidal recirculating zone. This phenomenon is characterized by the residence time of the gas between the two electrodes. Following [16], this residence time can be approximated by $\tau_{res} \approx d_p/u_{flow}$, where d_p is the diameter of the discharge channel and u_{flow} is the local flow velocity of the recirculating zone.

According to basic combustion theory [19,20], ignition will occur in the interelectrode region if the flow residence time τ_{res} is larger than the chemical reactions characteristic time scale τ_{chem}, i.e., if the Damköhler number $\mathrm{Da} = \tau_{res}/\tau_{chem}$ satisfies:

$$\mathrm{Da} > 1 \tag{1}$$

Although this condition is necessary, it may not be sufficient for plasma-assisted ignition, as it does not account for the successive interaction of pulses, required to accumulate a level of energy sufficient to activate combustion kinetics [5,12]. Such cumulative effect is possible only if the residence time τ_{res} is larger than the interpulse time, defined as $\tau_{ip} = 1/f_p$, i.e.

$$\tau_{res} > \tau_{ip} \tag{2}$$

Dividing each term of Eq. (2) by τ_{chem} and introducing $\Lambda = \tau_{ip}/\tau_{chem}$ leads to the following condition:

$$\mathrm{Da} > \Lambda \tag{3}$$

Therefore, ignition by NRP discharges is *a priori* possible only if conditions (2) and (3) are satisfied, i.e.

$$\mathrm{Da} > \max(1, \Lambda) \tag{4}$$

This coarse analysis has obvious flaws. Indeed, it reduces detailed chemistry phenomena to only one chemical characteristic time. In addition, for a given amount of discharge energy per pulse, it does not provide the number of pulses required to ignite. Finally, for a given value of the pulse repetition frequency, it does not indicate the minimum energy per pulse needed for ignition. To overcome these limitations, a model based on detailed chemistry computation of 0-D reactor configurations is introduced in the next section.

3. Low-order modeling of ignition by NRP discharges

3.1. Perfectly-stirred reactor model for plasma-assisted ignition

The present low-order model considers the volume surrounding the interelectrode region, illustrated in Fig. 2a, where the competition between plasma kinetics, combustion chemistry, and turbulent mixing occurs. The flow dynamic governs the amount of fresh gases flowing into the reactor, the rate of exhaust burnt gases, and the residence time τ_{res} of the gases inside this control volume. Interactions between mixing phenomena and plasma and combustion chemistry are modeled by considering a Perfectly-Stirred Reactor (PSR) as in [16], which is illustrated in Fig. 2b.

The time evolution of species mass fractions Y_k and specific mixture enthalpy h within the control volume is described by the classical conservation equations, Eqs. (5) and (6), governing the PSR to which sources related to plasma are added. These equations are completed by the conservation equation Eq. (7) for the vibrational energy e_{vib} introduced by plasma to the PSR in order to consider vibrational-translational relaxation.

$$\frac{dY_k}{dt} = \frac{1}{\tau_{res}}\left(Y_k^0 - Y_k\right) + \frac{W_k\dot{\omega}_k^c}{\rho} + \frac{W_k\dot{\omega}_k^p}{\rho} \tag{5}$$

$$\frac{dh}{dt} = \frac{1}{\tau_{res}}\left(\sum_{k=1}^{N_{sp}} Y_k^0 h_k^0 - \sum_{k=1}^{N_{sp}} Y_k h_k\right) + \frac{\dot{E}_{chem}^p}{\rho} + \frac{\dot{E}_{heat}^p}{\rho} + \frac{\dot{R}_{VT}^p}{\rho} \tag{6}$$

$$\frac{de_{vib}}{dt} = \frac{1}{\tau_{res}}\left(e_{vib}^0 - e_{vib}\right) + \frac{\dot{E}_{vib}^p}{\rho} - \frac{\dot{R}_{VT}^p}{\rho} \tag{7}$$

where the superscript 0 denotes fresh gases properties flowing in the PSR. In these equations τ_{res} is the residence time, and ρ the gas density.

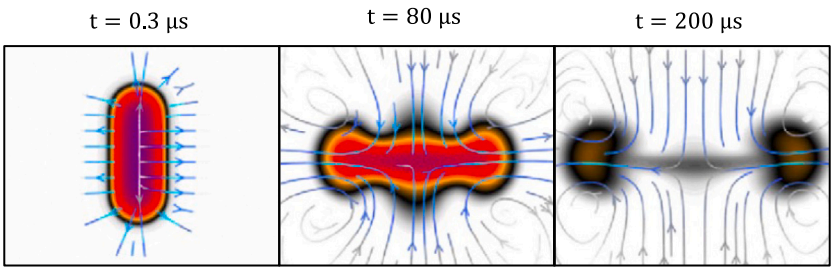

Fig. 1. Time evolution of the hot kernel morphology for $f_p = 5$ kHz and $E_p = 1.5$ mJ.
Source: Extracted from DNS of [15].

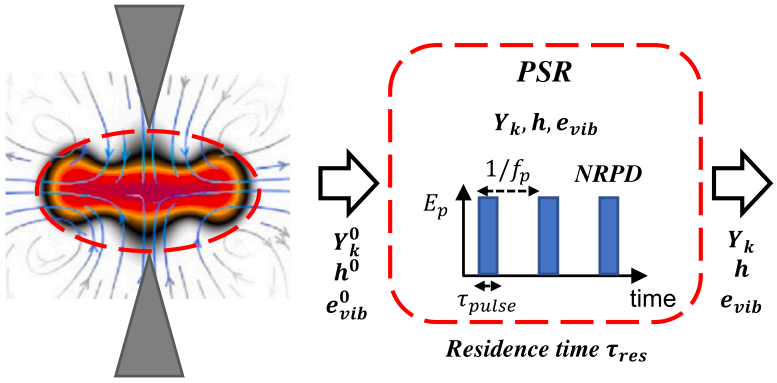

Fig. 2. (a) Flow recirculating in the discharge channel after a pulse. (b) PSR modeling of plasma-assisted ignition mechanism.
Source: Extracted and reproduced from [15,16].

h_k is the specific enthalpy of the kth species comprising a sensible and a chemical part: $h_k = h_{s,k} + \Delta h^0_{f,k}$. The rates $\dot{\omega}^c_k$ and $\dot{\omega}^p_k$ are the combustion and plasma chemistry source terms, respectively. The chemical and thermal rates of energy, $\dot{E}^p_{chem}$ and $\dot{E}^p_{heat}$, correspond to ultra-fast O_2 dissociation and gas heating due to plasma, respectively. $\dot{E}^p_{vib}$ is the vibrational rate of energy contributing to the vibrational excitation of N_2 due to plasma. $\dot{R}^p_{VT}$ is the vibrational-translational relaxation. All source terms related to plasma are presented in the next subsection.

3.2. Phenomenological modeling of NRP discharge

NRP spark discharges mainly induce an electronic and vibrational excitation of nitrogen molecules. The relaxation of nitrogen electronic states leads to an ultra-fast dissociation of O_2 molecules into O atoms and an increase of gas temperature at the nanosecond scale. In contrast, the relaxation of vibrational states causes a slow gas heating at the millisecond scale.

These processes are modeled by the semi-empirical strategy proposed by Castela et al. [21]. At each pulse, the discharge deposits a constant rate of energy $\dot{E}^p$ defined as:

$$\dot{E}^p = \begin{cases} \frac{E_p}{V_p \tau_{pulse}} & \text{if } t_{per} \leq \tau_{pulse} \\ 0 & \text{otherwise} \end{cases} \tag{8}$$

where $V_p = \pi r_p^2 L_p$ is the discharge volume (considered as quasi-cylindrical), $r_p = d_p/2$ the discharge radius, L_p the discharge length, τ_{pulse} the duration of a pulse, and t_{per} the time relative to the start of a pulse.

The rate of energy $\dot{E}^p$, deposited in the reactive mixture within the time τ_{pulse}, is split into three contributions:

$$\dot{E}^p = \dot{E}^p_{chem} + \dot{E}^p_{heat} + \dot{E}^p_{vib}. \tag{9}$$

These rates are modeled as the following:

$$\dot{E}^p_{chem} = \eta \frac{Y_{O_2}}{Y^0_{O_2}} \left(1 - \frac{e_{O_2}}{e_O}\right) \dot{E}^p \tag{10}$$

$$\dot{E}^p_{heat} = \left[\alpha - \eta \frac{Y_{O_2}}{Y^0_{O_2}} \left(1 - \frac{e_{O_2}}{e_O}\right)\right] \dot{E}^p \tag{11}$$

$$\dot{E}_{vib} = (1-\alpha)\dot{E}^p \tag{12}$$

where $Y^0_{O_2}$ is the mass fraction of O_2 in the fresh mixture; e_k is the specific internal energy of species; α is the fraction of pulse energy that induces the electronic excitation of N_2 and subsequently the ultra-fast gas heating and O_2 dissociation; η is the fraction of pulse energy involved directly into O_2 dissociation. Consequently, $(\alpha - \eta)$ is the fraction of energy deposited during ultra-fast heating, while $(1-\alpha)$ corresponds to the slow heating process.

According to experimental and theoretical characterization of NRP discharges [10,22], the parameters are here set to $\alpha = 55\%$ and $\eta = 35\%$. The ability of this NRP discharges model to reproduce the discharge effects (ultra-fast heating and O_2 dissociation, and slow heating) has been validated against measurements in [21].

The plasma chemistry source terms $\dot{\omega}^p_k$ are closed as in [21] by:

$$\dot{\omega}^p_O = \eta \frac{Y_{O_2}}{Y^0_{O_2}} \frac{\dot{E}^p}{e_O W_O} \tag{13}$$

$$\dot{\omega}^p_{O_2} = -\frac{W_O}{W_{O_2}} \dot{\omega}^p_O \tag{14}$$

$$\dot{\omega}^p_k = 0 \quad \text{if } k \neq \{O, O_2\}. \tag{15}$$

As for the vibrational-translational relaxation $\dot{R}^p_{VT}$, that leads to slow gas heating, is modeled with a Landau-Teller's harmonic oscillator [23]:

$$\dot{R}^p_{VT} = \rho \frac{e_{vib} - e^{eq}_{vib}(T)}{\tau_{VT}} \tag{16}$$

with the equilibrium value of the vibrational energy, at a given gas temperature T, defined by:

$$e^{eq}_{vib}(T) = \frac{\mathcal{R}\Theta_1 / W_{N_2}}{\exp(\Theta_1/T) - 1} \tag{17}$$

where $\mathcal{R}$ is the universal gas constant, W_{N_2} the molar mass of nitrogen molecules and $\Theta_1 = 3396$ K the vibrational temperature corresponding to the first quantum vibrational state of N_2. The vibrational-translational relaxation time τ_{VT} is computed as in [21] using experimental correlations from Milikan and White [24].

3.3. Validation of the low-order model

The 0D-PSR formulation is validated on a plasma-assisted ignition configuration investigated by Castela et al. [21]. The reference solution is given by the DNS of a methane-air mixture submitted to a series of NRP discharges in a 2-D Homogeneous Isotropic Turbulence (HIT) box. The mixture equivalence ratio is $\phi = 0.8$ and the reactant temperature and pressure are $T_i = 300$ K and $P_i = 1$ bar, respectively. The initial Reynolds number based on the integral scale is $\mathrm{Re}_t = l_t u'/\nu = 395$ where the velocity fluctuation is $u' = 6$ m.s^{-1} and the integral length scale $l_t = 6.25 \cdot 10^{-4}$ m. For the discharge parameters, the diameter is $d_p = 0.450$ mm, the length $L_p = 4$ mm, the pulse energy $E_p = 0.7$ mJ, the pulse repetition frequency $f_p = 10$ kHz, and the pulse duration $\tau_{pulse} = 50$ ns.

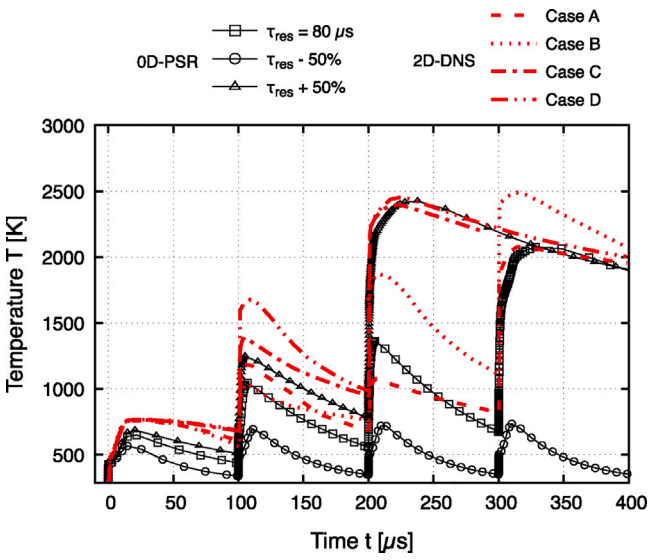

Fig. 3. Comparison of the gas temperature profile between 2D-DNS of Castela et al. (red lines) and 0D-PSR simulations of the present work (black lines), for the same conditions. (For interpretation of the references to color in this figure legend, the reader is referred to the web version of this article.)

The residence time of the gases in the plasma channel between the electrodes is estimated as $\tau_{res} \approx d_p/u' \approx 80$ µs. The simulations are performed with the 0D solver REGATH developed at EM2C laboratory [25]. The Lindstedt detailed mechanism for methane-air combustion, involving 29 species and 141 reactions [26] and used to obtain the reference DNS [21], is also retained for the 0D simulations.

The temporal evolution of gas temperature predicted by the low-order model is plotted in Fig. 3 (square black line) after a series of four pulses. The temperature gradually increases after each pulse until ignition occurs at about 300 µs. Results of the DNS simulations performed by [21] with the same NRP discharge model are shown by red lines. To mimic the chaotic nature of the turbulence four distinct DNS solutions (labeled A, B, C, D) are shown, which differ only by the initial HIT field. Two events leads to a ignition after 3 pulses while the other two require 4 pulses. The 0D model reproduces well the solutions from events A and B, but does not have enough degree of freedom to capture the other events. Assuming that the different turbulent realizations can be captured by adding an uncertainty in the residence time, two supplementary solutions, corresponding to $\tau_{res} \pm 50\%$ are added to Fig. 3 (circle and triangle black lines). Interestingly, the solution obtained by $\tau_{res} + 50\%$ is now closer to events C and D.

There is therefore a great sensibility to the residence time parameter in the early stage of plasma-assisted ignition. While difficult to *a priori* estimate in practice, it is however a relevant quantity for a parametric study.

4. Numerical set-up

For all the studied cases, the PSR is initialized and fed by a fresh methane-air mixture of equivalence ratio $\phi = 0.95$ and temperature $T^0 = 300$ K under atmospheric pressure conditions. For each simulation, the computed physical time reaches 10 ms. The GRI-Mech 3.0 detailed kinetics scheme involving 53 species and 325 reactions is used for the combustion mechanism of methane-air [27]. Concerning the NRPD model, the discharge diameter and length are fixed at $d_p = 1.75$ mm and $L_p = 5$ mm, respectively, and the duration of a pulse is fixed at $\tau_{pulse} = 50$ ns [16].

Fig. 4 presents a typical temporal evolution of temperature and methane mass fraction for a pulse repetition frequency of $f_p = 20$ kHz, an energy per pulse of $E_p = 3.5$ mJ, and a residence time of $\tau_{res} = 0.5$ ms.

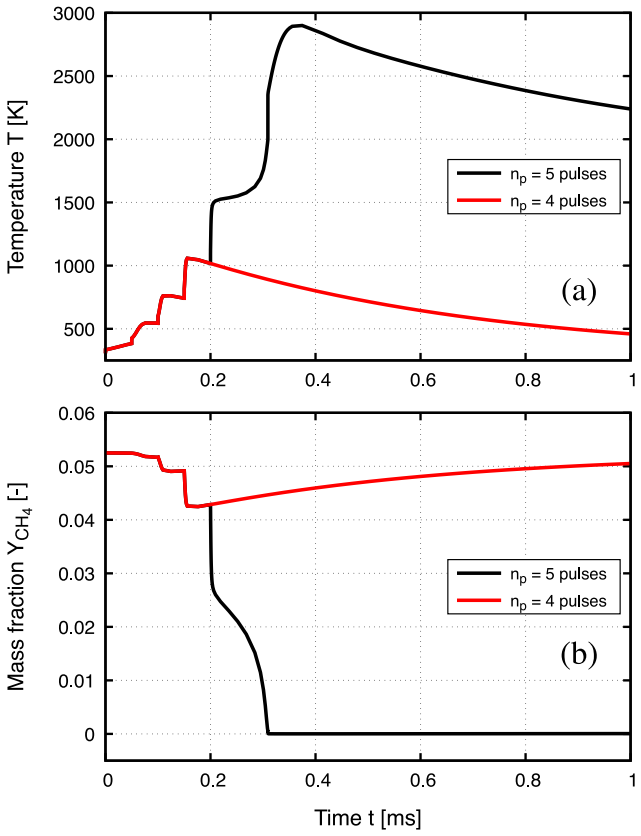

Fig. 4. Typical temporal profiles of (a) temperature and (b) methane mass fraction for $f_p = 20$ kHz, $E_p = 3.5$ mJ, and $\tau_{res} = 0.5$ ms. Black profiles are obtained by applying five discharge pulses and red profiles by four discharge pulses. (For interpretation of the references to color in this figure legend, the reader is referred to the web version of this article.)

The black profiles are obtained by applying a burst of five discharges, which is enough to increase the gas temperature to about 1500 K, where chain-branching reactions take place, ignition occurs, and the methane entering the reactor is entirely consumed. Then, the temperature passes through a maximum and reaches a steady state at about 10 ms.

If one applies only four discharge pulses (red profiles) for the same operating conditions, the temperature will not get high enough to produce enough radicals to ignite the mixture. As the fresh mixture is permanently injected into the PSR, temperature decreases to the inlet temperature ($T^0 = 300$ K), and methane mass fraction goes up to its initial value ($Y^0_{CH_4} = 0.0525$ for $\phi = 0.95$). For these conditions, the ignition delay time, defined as the time needed to consume 99% of CH_4, is $\tau_{ign} = 3.1$ ms, and the corresponding minimum number of pulses n_p needed to ignite the reactor is five.

A parametric study is now conducted on this 0-D configuration by varying the amount of deposited energy per pulse E_p and the pulse repetition frequency f_p. First, for $f_p = 20$ kHz, ten values of E_p between 0.5 and 5 mJ with an increment of 0.5 mJ have been examined. Then, for $E_p = 3.5$ mJ, nine frequencies ($f_p = 1$, 2, 3.5, 6, 10, 20, 35, 60, and 100 kHz) have been examined.

5. Results and discussions

5.1. Effect of pulse energy E_p

In this section, the effect of pulse energy on the ignition process is investigated for various residence times. The pulse repetition frequency is kept constant to $f_p = 20$ kHz.

The minimum number of pulses required to ignite the reactor is first plotted as a function of the residence time in Fig. 5a for $E_p = 3.5$ mJ. As expected, the number of pulses increases when τ_{res} decreases. For $\tau_{res} < 0.4$ ms, a sharp increase of the number of pulses is observed, exhibiting a critical residence time limit of $\tau_{res}^{crit} = 0.08$ ms, below which ignition cannot occur. For 0.4 ms $< \tau_{res} <$ 5 ms, a plateau is observed with $n_p = 5$ and then n_p decreases to 4 when $\tau_{res} > 5$ ms.

Fig. 5b and c present the temporal profiles of temperature for the four residence times indicated in Fig. 5a. For $\tau_{res} = 0.1$ ms (see Fig. 5b), just above $\tau_{res}^{crit} = 0.08$ ms, $n_p = 15$ pulses are needed to ignite the flame and the corresponding ignition delay is $\tau_{ign} = 0.7$ ms. When τ_{res} is slightly increased to 0.3 ms, the minimum number of pulses drastically decreases to $n_p = 6$ (and $\tau_{ign} = 0.26$ ms). For a much higher residence time of $\tau_{res} = 5$ ms (see Fig. 5c), $\tau_{ign} = 0.2$ ms has the same order of magnitude as for $\tau_{res} = 0.3$ ms. When the residence times is changed from $\tau_{res} = 5$ ms to $\tau_{res} = 6$ ms, the minimum number of pulses needed for ignition decreases from $n_p = 5$ to $n_p = 4$ and the ignition delay τ_{ign} significantly increases to 2.3 ms.

Fig. 6a presents the evolution of the minimum number of pulses n_p needed to ignite the fresh gases for $E_p = 5.0$ mJ and $f_p = 20$ kHz. An evolution similar to Fig. 5a is observed. However, an extensive analysis of the time evolution of thermodynamic variables shows the existence of a region where the ignition occurs but is then followed by an extinction. Every value of τ_{res} was checked to identify ignited-extinct cases from fully ignited ones. This phenomenon is visible in the time evolution of temperature and methane mass fraction, plotted in Fig. 6b and c, respectively. For the intermediate value of $\tau_{res} = 0.07$ ms, even if the discharges can ignite the gases at about $t = 0.75$ ms, the residence time is too short and the temperature increase is not sufficient to produce enough active radicals to maintain the combustion, while at the same time, fresh gases continuously enter the burner and decrease the temperature. An intermediate zone is hence observed where the flow dynamics and the combustion complex chemistry compete. Indeed, at about $t = 1.05$ ms, the temperature decreases and chemical reactions stop while fresh gases continue to flow into the burner. Consequently, the gas temperature reaches that of the fresh mixture and the mass fraction of CH_4 reaches its initial value.

The minimum number of pulses n_p is now plotted as a function of the residence time τ_{res} for different values of pulse energy E_p in Fig. 7a. A behavior similar to Fig. 5a is observed, whatever the amount of energy per pulse E_p is applied. As expected, the critical residence time τ_{res}^{crit} increases when decreasing E_p. Fig. 8a plots the evolution of n_p, in terms of the energy per pulse at two residence times. The number of pulses needed to ignite decreases when E_p increases for both low ($\tau_{res} = 0.1$ ms) and high ($\tau_{res} = 2$ ms) residence times.

The total deposited energy required for ignition, $E_p^{tot} = n_p E_p$, is presented in Fig. 7b as a function of the residence time. For residence times lower than $\tau_{res} = 0.4$ ms, the total amount of deposited energy decreases when the energy per pulse E_p increases.

This is also visible in Fig. 8b which shows the total deposited energy as a function of the energy per pulse. At $\tau_{res} = 0.1$ ms, a total deposited energy of $E_p^{tot} = 84$ mJ is needed for $E_p = 3$ mJ, while only 35 mJ are required for $E_p = 5$ mJ. In addition, the ignition delay, shown in Fig. 7c, also decreases when E_p increases. Therefore, increasing the energy per pulse at low residence times appears to be more efficient in igniting the mixture. In fact, the increase of deposited energy per pulse sufficiently enhances chemical activity to overcome short residence time of the gases in the reactor.

Interestingly, Fig. 7b shows an opposite behavior for residence times higher than $\tau_{res} \approx 0.7$ ms. The total deposited energy now increases when the energy per pulse increases. For instance, Fig. 8b shows that at $\tau_{res} = 2$ ms a total deposited energy of $E_p^{tot} = 12$ mJ is needed

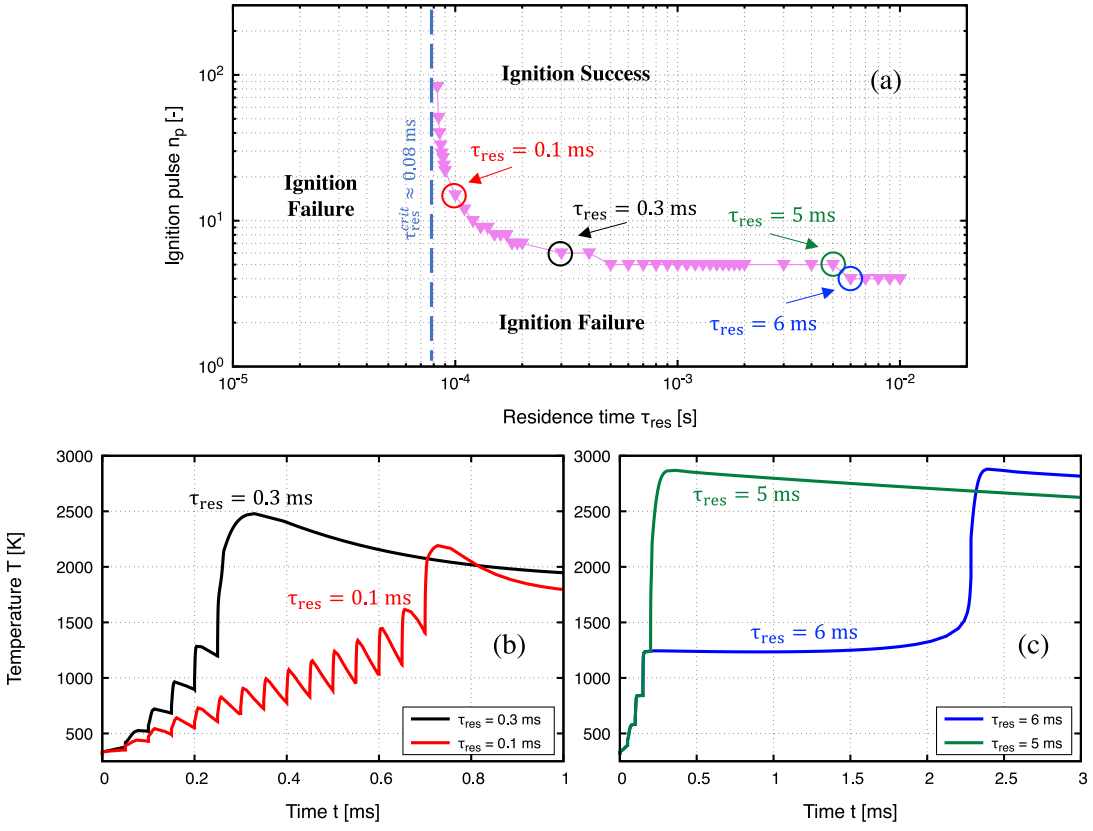

Fig. 5. (a) Minimum number of pulses n_p required to ignite the methane-air mixture ($\phi = 0.95$) as a function of the residence time τ_{res}. Temporal evolution of temperature (b) for two residence times of $\tau_{res} = 0.1$ and 0.3 ms, and (c) for two residence times of $\tau_{res} = 5$ and 6 ms. The pulse energy and the pulse repetition frequency are, respectively, fixed at $E_p = 3.5$ mJ and $f_p = 20$ kHz.

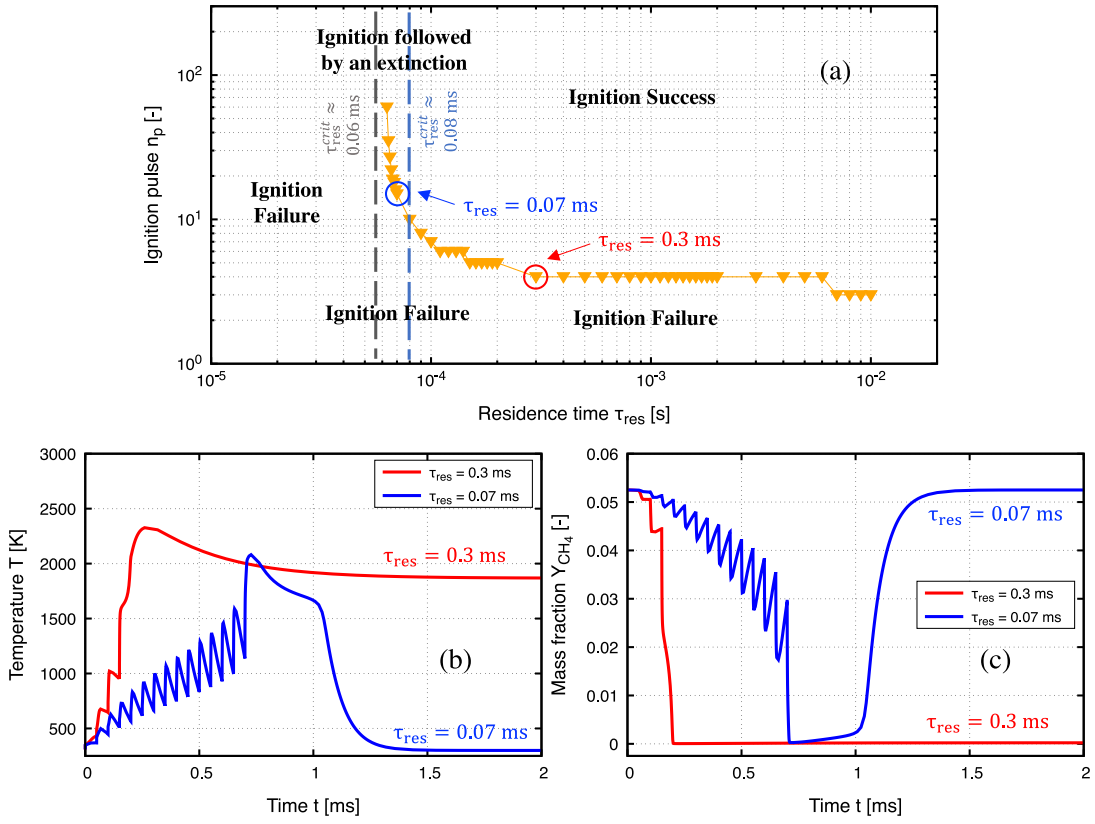

Fig. 6. (a) Minimum number of pulses n_p required to ignite the methane-air mixture ($\phi = 0.95$) as a function of the residence time τ_{res} for a pulse energy of $E_p = 5.0$ mJ and a pulse repetition frequency of $f_p = 20$ kHz. Temporal evolution of (b) temperature and (c) methane mass fraction for two residence times of $\tau_{res} = 0.07$ and 0.3 ms.

for $E_p = 1$ mJ, while 20 mJ are required for $E_p = 5$ mJ. However, similarly to what was observed at low residence times, the ignition delay increases when the energy per pulse (and consequently the total deposited energy) decreases (see Fig. 8c). In this condition, less energy is needed to ignite the mixture, but with a longer delay. In fact, the decrease of deposited energy per pulse slows down chemical activity. However, as the residence time is long enough, the chain-branching reactions produce enough radicals to ignite the mixture.

The simplified theory present in Section 2 will now be challenged against the results of the low-order model obtained in the current section. The Damköhler number $\mathrm{Da}^{crit} = \tau_{res}^{crit}/\tau_{chem}$ is computed from the critical residence time τ_{res}^{crit}, estimated from the PSR simulations. τ_{res}^{crit} corresponds to the minimum residence time for which ignition occurs and leads to a burning steady-state regime, at a given E_p and f_p. The chemical time scale defined as:

$$\tau_{chem} = \left(\max \left| \frac{\dot{\omega}_{\mathrm{CH_4}}^{c}}{\rho} \right| \right)^{-1} . \tag{18}$$

Ignition occurs only when $\mathrm{Da} > \mathrm{Da}^{crit}$. The black squares in Fig. 9 show the evolution of Da^{crit} as a function of pulse energy E_p for $f_p = 20$ kHz. The limit given by $\Lambda = \tau_{ip}/\tau_{chem}$ shown by the red circles in this figure, significantly underestimates Da^{crit}, especially for low values of E_p. The horizontal blue-dashed line in Fig. 9 shows a second limit, given by $\mathrm{Da} = 1$. This limit is very close to the reference one, $\mathrm{Da} = \mathrm{Da}^{crit}$. These observations imply that the chemical time is here more restrictive than the interpulse time. Therefore, the condition $\mathrm{Da} > \max(1, \Lambda)$ is, in general, well respected when ignition occurs except for very low values of E_p. This can be attributed to the approximation of the chemical time scale by Eq. (18), where only one species has been considered.

5.2. Effect of pulse repetition frequency f_p

In this section, the effect of pulse repetition frequency f_p on the ignition process is investigated. The pulse energy is kept constant, $E_p = 3.5$ mJ.

Similarly to the study of pulse energy presented in Section 5.1, the minimum number of pulses n_p, the minimum total deposited energy E_p^{tot}, and ignition delay τ_{ign} are represented in Fig. 10 in terms of the gas residence time τ_{res} for different pulse repetition frequencies f_p. By increasing the frequency f_p, the minimum number of pulses needed to ignite the mixture and the corresponding total deposited energy E_p^{tot} decrease and ignition becomes more efficient, moving the critical residence time τ_{res}^{crit} towards smaller values. At high values of the residence times τ_{res}, as in Fig. 7a, a plateau is observed with very low variation of $n_p = 5$. The ignition delay also shows the same behavior as in Fig. 7c.

Fig. 11 shows the evolution of the minimum number of pulses n_p, the corresponding total deposited energy E_p^{tot} and the ignition delay τ_{ign} in terms of pulse repetition frequency f_p for two values of the residence time. At the small value of the residence time $\tau_{res} = 0.1$ ms, by increasing the pulse repetition frequency, n_p, E_p^{tot}, and τ_{ign} decrease. However, for the large value of the residence time $\tau_{res} = 2$ ms, the minimum number of pulses n_p and the corresponding total deposited energy E_p^{tot} required for ignition remain rather constant, while the ignition delay τ_{ign} decreases when f_p increases.

Finally, similarly to the study of pulse energy presented in Section 5.1, the simplified theory present in Section 2 will also be challenged against the results of the low-order model obtained in the current section. The Damköhler number Da^{crit} is computed from the critical residence time τ_{res}^{crit}, estimated from the PSR simulations. The chemical time scale is still computed with Eq. (18). Ignition occurs only when $\mathrm{Da} > \mathrm{Da}^{crit}$. The black squares, in Fig. 12, shows the evolution of

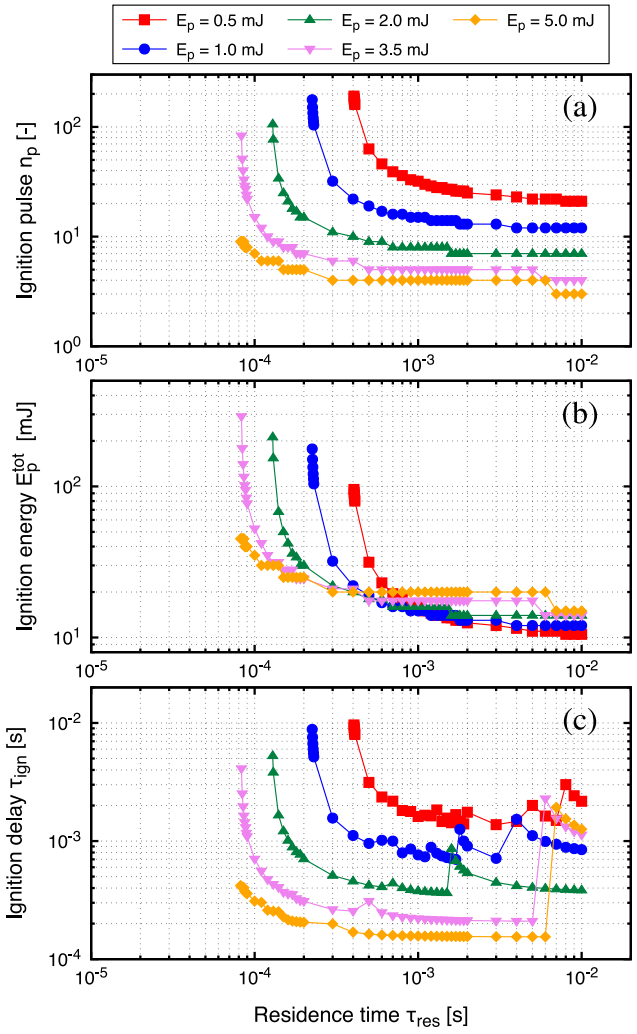

Fig. 7. Plasma-assisted ignition diagrams. (a) Number of pulses n_p, (b) total deposited energy E_p^{tot}, and (c) ignition delay time τ_{ign} required to ignite the methane-air mixture ($\phi = 0.95$) in terms of the residence time τ_{res} for various pulse energy E_p. The pulse repetition frequency is fixed at $f_p = 20$ kHz.

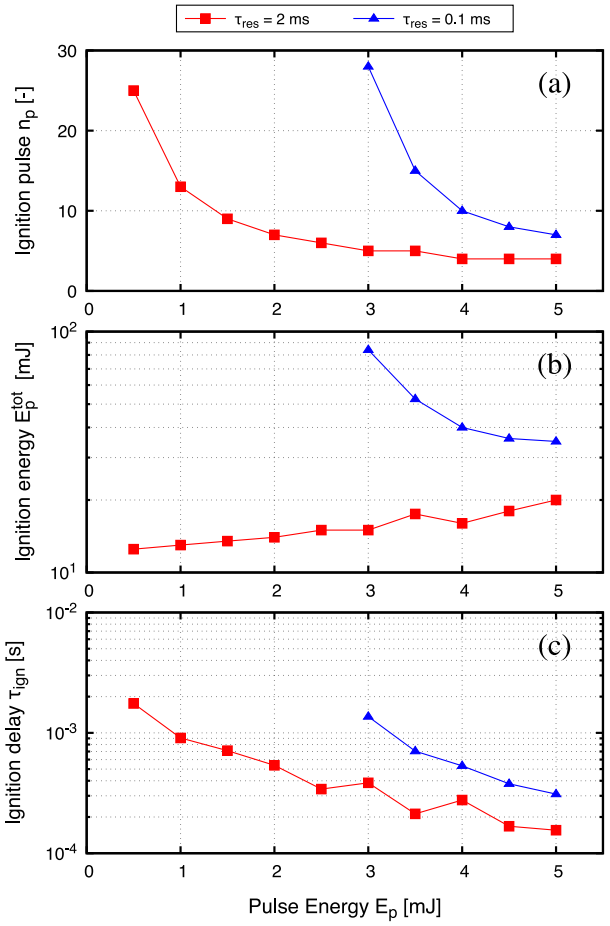

Fig. 8. Effect of pulse energy E_p on (a) number of pulses n_p, (b) total deposited energy E_p^{tot}, and (c) ignition delay τ_{ign} for two residence times $\tau_{res} = 0.1$ and 2 ms. $f_p = 20$ kHz. The pulse repetition frequency is fixed at $f_p = 20$ kHz.

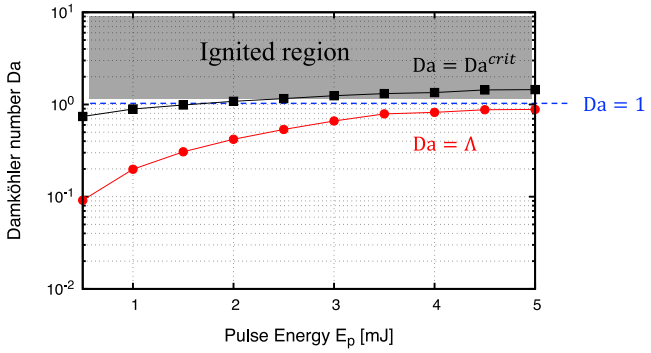

Fig. 9. Evolution of the Damköhler number Da as a function of pulse energy E_p for a constant pulse repetition frequency $f_p = 20$ kHz; Da^{crit} corresponding to the critical residence time τ_{res}^{crit} (black squares), Da = 1 corresponding the characteristic chemical time τ_{chem} at this residence time (blue-dashed line), and Λ corresponding to interpulse time τ_{ip} (red circles). The gray area is the Da > max(1, Λ) condition region. (For interpretation of the references to color in this figure legend, the reader is referred to the web version of this article.)

Da^{crit} in terms of pulse repetition frequency f_p for $E_p = 3.5$ mJ. The limit given by $\Lambda = \tau_{ip}/\tau_{chem}$ shown by the red circles in this figure, significantly underestimates Da^{crit}, especially for low values of E_p. The horizontal blue-dashed line and the red circles show the limits given by Da = 1 and Da = Λ, respectively.

When $f_p < 10$ kHz, $\Lambda > 1$ and the ignition criteria is given by Da > Λ. This is consistent with the observation made in Fig. 12, as the Da = Λ line is the closest to Da^{crit}. Inversely, when $f_p > 10$ kHz, $\Lambda < 1$ and the ignition constraint is given by Da > 1. These observations imply that the chemical time is here more restrictive for values of $f_p > 10$ kHz. In contrast, interpulse time is the more restrictive one for values of $f_p < 10$ kHz. Therefore, here also, the condition Da > max(1, Λ) is well respected when ignition occurs.

6. Conclusions

Following [16], a low-order model of flame ignition by NRP discharges has been used to analyze the ignition success or failure of a methane-air mixture in a perfectly-stirred reactor. The PSR represents the volume surrounding the interelectrode region where the competition between plasma kinetics, combustion chemistry, and turbulent mixing occurs. Ignition success or failure results from a competition between the cumulative energy deposited in the PSR, which affects the combustion chemistry, the residence time of gases and the inter pulse time. A parametric study is performed in this 0-D configuration by varying the amount of deposited energy per pulse E_p and the pulse repetition frequency f_p to obtain diagrams giving the ignition limits and the efficient operating conditions.

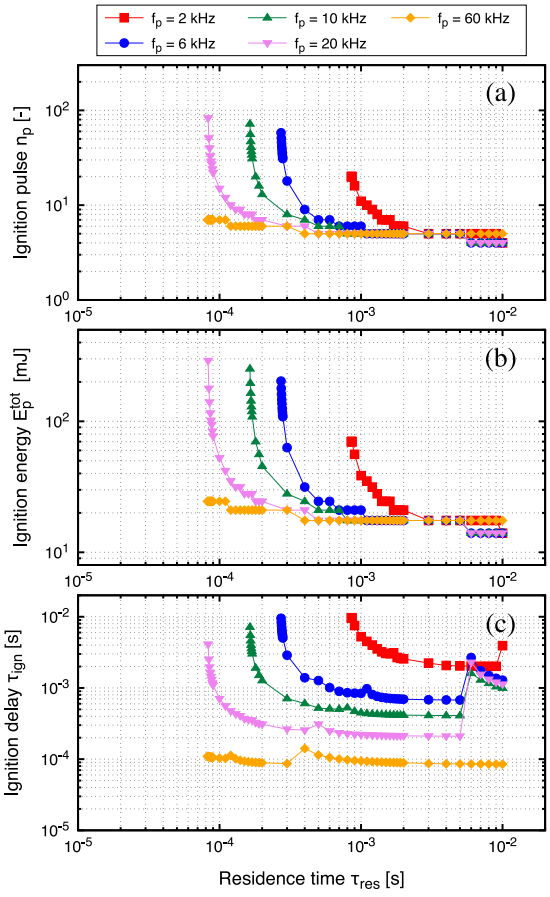

Fig. 10. Plasma-assisted ignition diagrams. (a) Number of pulses n_p, (b) total deposited energy E_p^{tot}, and (c) ignition delay time τ_{ign} required to ignite the methane-air mixture ($\phi = 0.95$) in terms of the residence time τ_{res} for various pulse repetition frequency f_p. The pulse energy is fixed at $E_p = 3.5$ mJ.

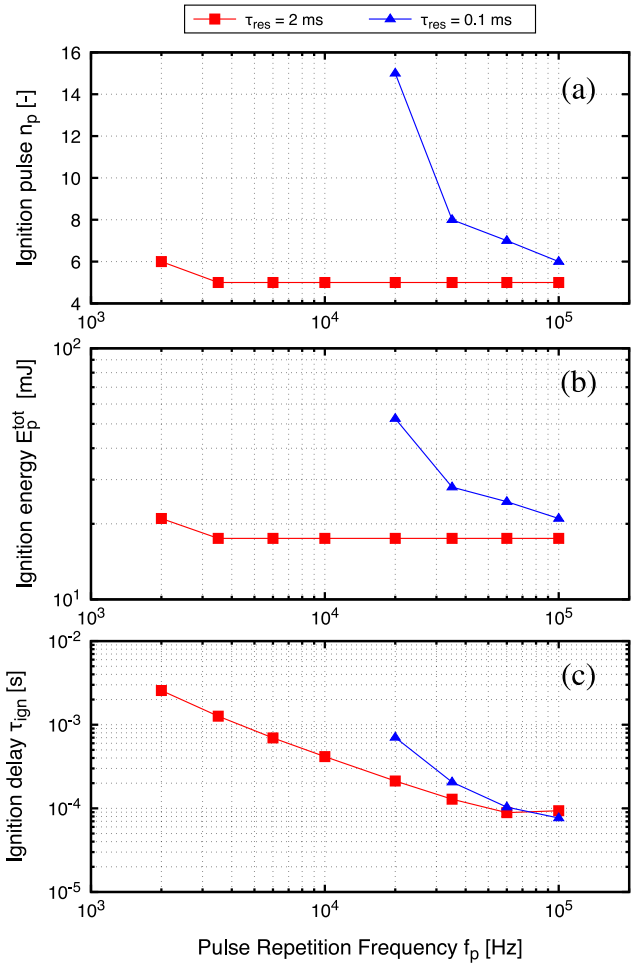

Fig. 11. Effect of pulse frequency f_p on (a) number of pulses n_p, (b) total deposited energy E_p^{tot}, and (c) ignition delay τ_{ign} for two residence times $\tau_{res} = 0.1$ and 2 ms. The pulse energy is fixed at $E_p = 3.5$ mJ.

At a fixed value of pulse energy E_p and pulse repetition frequency f_p, the minimum number of pulses needed to ignite the gas mixture increases when τ_{res} decreases. For very low values of τ_{res}, a sharp increase in the number of pulses n_p is observed, exhibiting a critical residence time τ_{res}^{crit} limit below which ignition cannot occur. This limit is extended when increasing whether the pulse energy E_p or the pulse repetition frequency f_p. In addition, for both low and high residence times, the number of pulses n_p and the ignition delay τ_{ign} decrease when increasing the energy deposited per pulse E_p.

At a fixed value of pulse frequency f_p, for high residence times, the total deposited energy E_p^{tot} increases with E_p, while for low residence times, it decreases with E_p. At a fixed value of pulse energy E_p, for low residence times, the total deposited energy E_p^{tot} decrease with f_p, while for high residence times, it remains relatively constant with f_p.

A simplified theory of plasma-assisted ignition based on dimensionless numbers constructed from the residence time τ_{res}, the interpulse one τ_{ip}, and the chemical one τ_{chem}, has been proposed. The analysis of the PSR solutions, using this simplified theory, showed that the condition $\mathrm{Da} > \max(1, \Lambda)$ on the Damköhler number Da is a good criterion to indicate that:

- the burst of discharges leads to a successful ignition
- the ignited mixture reaches a burning steady state regime

The respect of these two conditions promotes the formation of a reactive kernel, making a turbulent flame ignition possible. Future works will concern the introduction of molecular diffusion effects in the low-order model, which may have a significant impact of the plasma-assisted ignition process.

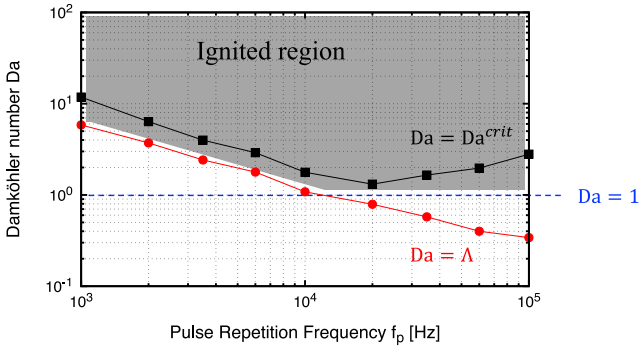

Fig. 12. Evolution of the Damköhler number Da as a function of pulse repetition frequency f_p constant pulse energy $E_p = 3.5$ mJ; Da^{crit} corresponding to the critical residence time τ_{res}^{crit} (black squares), $\mathrm{Da} = 1$ corresponding to the characteristic chemical time at this residence time τ_{chem} (blue-dashed line), and Λ corresponding to interpulse time τ_{ip} (red circles). The gray area is the $\mathrm{Da} > \max(1, \Lambda)$ condition region. (For interpretation of the references to color in this figure legend, the reader is referred to the web version of this article.)

Declaration of competing interest

The authors declare that they have no known competing financial interests or personal relationships that could have appeared to influence the work reported in this paper.

Data availability

Data will be made available on request

Acknowledgments

This research was funded by the PASTEC project of the French Agence Nationale de la Recherche (ANR) (Grant No. ANR-16-CE22-0005) and the GREENBLUE project of the European Research Council (ERC) under the European Union's Horizon 2020 programme (Grant No. 101021538). A CC-BY public copyright license has been applied by the authors to the present document and will be applied to all subsequent versions up to the Author Accepted Manuscript arising from this submission, in accordance with the grant's open access conditions. This work was performed using HPC resources from the "Mésocentre" computing center of CentraleSupélec, École Normale Supérieure Paris-Saclay and Université Paris-Saclay supported by CNRS and Région Île-de-France. The authors would like to thank Christophe O. Laux, Victorien P. Blanchard, and Jean-Baptiste Perrin-Terrin for insightful discussions on plasma-assisted combustion/ignition.

References

[1] Ju Y, Sun W. Plasma assisted combustion: Dynamics and chemistry. Prog Energy Combust Sci 2015;48:21–83. http://dx.doi.org/10.1016/j.pecs.2014.12.00.

[2] Starikovskiy A, Aleksandrov N. Plasma-assisted ignition and combustion. Prog Energy Combust Sci 2013;39(1):61–110. http://dx.doi.org/10.1016/j.pecs.2012.05.003.

[3] Galley D, Pilla G, Lacoste D, Ducruix S, Lacas F, Veynante D, Laux CO. Plasma-enhanced combustion of a lean premixed air-propane turbulent flame using a nanosecond repetitively pulsed plasma. In: 43rd AIAA Aerospace Sciences Meeting. Reno, Nevada, USA; 2005, p. 1193. http://dx.doi.org/10.2514/6.2005-1193.

[4] Pilla G, Galley D, Lacoste DA, Lacas F, Veynante D, Laux CO. Stabilization of a turbulent premixed flame using a nanosecond repetitively pulsed plasma. IEEE Trans Plasma Sci 2006;34(6):2471–7. http://dx.doi.org/10.1109/TPS.2006.886081.

[5] Xu DA, Lacoste DA, Laux CO. Ignition of quiescent lean propane–air mixtures at high pressure by nanosecond repetitively pulsed discharges. Plasma Chem Plasma Process 2016;36:309–27. http://dx.doi.org/10.1007/s11090-015-9680-3.

[6] Macheret S, Shneider M, Miles R. Energy efficiency of plasma-assisted combustion in ram/scramjet engines. In: 36th AIAA Plasmadynamics and Lasers Conference. Toronto, Ontario, Canada; 2005, p. 5371. http://dx.doi.org/10.2514/6.2005-5371.

[7] Li S, Bai C, Chen X, Meng W, Li L, Pan J. Numerical investigation on plasma assisted ignition of methane/air mixture excited by the synergistic nanosecond repetitive pulsed and DC discharge. J Phys D: Appl Phys 2020;54(1):015203. http://dx.doi.org/10.1088/1361-6463/abb8ae.

[8] Bai C, Li S, Chen T, Chen X, Meng W, Pan J. Methane–air plasma-assisted ignition excited by nanosecond repetitively pulsed discharge: Numerical modeling and effect of inert gas. ACS Omega 2021;6(37):24156–65. http://dx.doi.org/10.1021/acsomega.1c03696.

[9] Barleon N, Cheng L, Cuenot B, Vermorel O, Bourdon A. Investigation of the impact of NRP discharge frequency on the ignition of a lean methane-air mixture using fully coupled plasma-combustion numerical simulations. Proc Combust Inst 2023;39(4):5521–30. http://dx.doi.org/10.1016/j.proci.2022.07.046.

[10] Rusterholtz DL, Lacoste DA, Stancu GD, Pai DZ, Laux CO. Ultrafast heating and oxygen dissociation in atmospheric pressure air by nanosecond repetitively pulsed discharges. J Phys D: Appl Phys 2013;46(46):464010. http://dx.doi.org/10.1088/0022-3727/46/46/464010.

[11] Lo A, Cessou A, Boubert P, Vervisch P. Space and time analysis of the nanosecond scale discharges in atmospheric pressure air: I. Gas temperature and vibrational distribution function of N2 and O2. J Phys D: Appl Phys 2014;47(11):115201. http://dx.doi.org/10.1088/0022-3727/47/11/115201.

[12] Lefkowitz JK, Ombrello T. An exploration of inter-pulse coupling in nanosecond pulsed high frequency discharge ignition. Combust Flame 2017;180:136–47. http://dx.doi.org/10.1016/j.combustflame.2017.02.032.

[13] Lefkowitz JK, Ombrello T. Reduction of flame development time in nanosecond pulsed high frequency discharge ignition of flowing mixtures. Combust Flame 2018;193:471–80. http://dx.doi.org/10.1016/j.combustflame.2018.04.009.

[14] Lefkowitz JK, Hammack SD, Carter CD, Ombrello TM. Elevated OH production from NPHFD and its effect on ignition. Proc Combust Inst 2021;38(4):6671–8. http://dx.doi.org/10.1016/j.proci.2020.09.002.

[15] Castela M, Stepanyan S, Fiorina B, Coussement A, Gicquel O, Darabiha N, Laux CO. A 3-D DNS and experimental study of the effect of the recirculating flow pattern inside a reactive kernel produced by nanosecond plasma discharges in a methane-air mixture. Proc Combust Inst 2017;36(3):4095–103. http://dx.doi.org/10.1016/j.proci.2016.06.174.

[16] Bechane Y, Fiorina B. Numerical investigations of turbulent premixed flame ignition by a series of Nanosecond Repetitively Pulsed discharges. Proc Combust Inst 2021;38(4):6575–82. http://dx.doi.org/10.1016/j.proci.2020.06.258.

[17] Pai DZ, Lacoste DA, Laux CO. Transitions between corona, glow, and spark regimes of nanosecond repetitively pulsed discharges in air at atmospheric pressure. J Appl Phys 2010;107(9):093303. http://dx.doi.org/10.1063/1.3309758.

[18] Minesi N, Stepanyan S, Mariotto P, Stancu GD, Laux CO. Fully ionized nanosecond discharges in air: the thermal spark. Plasma Sources Sci Technol 2020;29(8):085003. http://dx.doi.org/10.1088/1361-6595/ab94d3.

[19] Peters N. Turbulent combustion. Cambridge University Press; 2000.

[20] Poinsot T, Veynante D. Theoretical and numerical combustion. third ed.. 2011,

[21] Castela M, Fiorina B, Coussement A, Gicquel O, Darabiha N, Laux CO. Modelling the impact of non-equilibrium discharges on reactive mixtures for simulations of plasma-assisted ignition in turbulent flows. Combust Flame 2016;166:133–47. http://dx.doi.org/10.1016/j.combustflame.2016.01.009.

[22] Popov N. Fast gas heating initiated by pulsed nanosecond discharge in atmospheric pressure air. In: 51st AIAA Aerospace Sciences Meeting. Grapevine, Texas, USA; 2013, p. 1052. http://dx.doi.org/10.2514/6.2013-1052.

[23] Landau L, Teller E. Theory of monomolecular reactions. Phys Z Sowjetunion 1936;10:34.

[24] Milikan RC, White DR. Systematics of vibrational relaxation. J Chem Phys 1963;39(12):3209–13. http://dx.doi.org/10.1063/1.1734182.

[25] Darabiha N. Transient behaviour of laminar counterflow hydrogen-air diffusion flames with complex chemistry. Combust Sci Technol 1992;86(1–6):163–81. http://dx.doi.org/10.1080/00102209208947193.

[26] Lindstedt P. Modeling of the chemical complexities of flames. Symp (Int) Combust 1998;27(1):269–85. http://dx.doi.org/10.1016/S0082-0784(98)80414-1.

[27] Smith GP, Golden DM, Frenklach M, Moriarty NW, Eiteneer B, Goldenberg M, Bowman CT, Hanson RK, Song S, Gardiner WC, Lissianski VV, Qin Z. http://www.me.berkeley.edu/gri_mech/.